

Adaptive diving depth control system for the drifting autonomous underwater vehicle

Viktor Ivel, Yuliya Gerasimova, Sayat Moldakhmetov, Makhabbat Krivolapova

Department of Energetic and Radioelectronics, Faculty of Engineering and Digital Technology, M. Kozybayev North-Kazakhstan University, Petropavlovsk, Kazakhstan

Article Info

Article history:

Received Dec 14, 2023

Revised Sep 17, 2024

Accepted Sep 20, 2024

Keywords:

Adaptive control

Autonomous vehicle

Diving depth

Parametric identification

Underwater vehicle

ABSTRACT

This article considers the system for controlling the diving depth of a drifting autonomous underwater vehicle (DAUV), which navigates underwater under the influence of sea currents in order to collect scientific information. The paper solves the problem of identifying non-stationary hydrodynamic parameters of the DAUV with the aim of adaptive adjustment of the DAUV control algorithm to increase the accuracy of bringing the DAUV to a given depth and minimizing the consumption of electricity consumed by power actuators. The solution to the problem is based on the use of parametric identification apparatus and adaptive control principles. The high quality of the DAUV diving depth control is achieved through the use of the method of adaptive adjustment of the parameters of the DAUV program model. The use of parametric identification of the hydrodynamic parameters of the DAUV made it possible to quickly adjust the corrective link in the control chain of the executing mechanism of the DAUV. The developed computer models and a set of semi-realistic tests made it possible to choose the most acceptable identification algorithm and configure the software implementation of the DAUV diving depth control law.

This is an open access article under the [CC BY-SA](https://creativecommons.org/licenses/by-sa/4.0/) license.



Corresponding Author:

Makhabbat Krivolapova

Department of Energetic and Radioelectronics, Faculty of Engineering and Digital Technology

M. Kozybayev North-Kazakhstan University

Str. Pushkin 86, 150000 Petropavlovsk, North Kazakhstan, Republic of Kazakhstan

Email: krivolapova_m@ptr.nis.edu.kz

1. INTRODUCTION

The study of sea currents, including the measurement of physical and chemical parameters of water, belongs to the category of applied tasks, the solution of which is a priority in the development of science and technology in many developed countries worldwide. Underwater vehicles and underwater robots are effective tools that allow the successful solution to the problems of world ocean development [1]. The analysis of global trends in the development of underwater instrumentation indicates the increasing pace of development of new generation underwater vehicles and robots based on the achievements of fundamental sciences and modern computer technologies that allow the creation of optimal control systems for the spatial movement of vehicles and robots in the aquatic environment according to various criteria [2]-[4]. In this paper, two problems are considered, the solution of which will ensure a high level of quality of automatic autonomous underwater vehicle control. The first problem includes the bringing of the drifting autonomous underwater vehicle (DAUV) to a given depth and its stabilization at this depth. The second one concerns minimizing energy consumption.

The theoretical foundations of modern underwater instrumentation were specified in [5], which describes the methods of analysis and calculation of kinematic and dynamic parameters of the main types of uncontrolled underwater vehicle movements. This work also includes a detailed description of the methods of

hydrodynamic forces acting on the underwater vehicle and a mathematical description of the most typical steady and unsteady movements of the vehicles. Although the paper did not address the issues of controlling the movement of the DAUV, the dynamic model of the spatial movement of the DAUV, which includes complex nonlinear differential equations with variable parameters, still serves as the basis for the design and research of underwater vehicles and robots for various purposes.

The issues of autonomous underwater vehicle (AUV) control under the conditions of uncertainty of individual parameters of the dynamic AUV model are considered in [6]. There are presented results of using the robust backstopping technique for organizing a recursive procedure in which the problems of finding the Lyapunov function and the corresponding control law are combined. The design of feedback control is done in such a way that the Lyapunov function has certain properties that guarantee convergence to an equilibrium point.

The works [7], [8] summarize the experience of designing self-propelled autonomous underwater vehicles for the exploration and development of the World Ocean. Methods for calculating the hydrodynamics and strength of hull structures and a propulsive complex, as well as navigation and orientation systems, motion control and positioning are given there. The papers also include a detailed description of the mass-dimensional and energy properties of the systems that are part of the DAUV and determine its technical characteristics, as well as the main aspects of DAUV development and their systems forming a specific DAUV design in accordance with the design assignment. The research onboard units and information processing equipment are described. The calculation methods and mathematical models presented in [7], [8] were fully taken into account in the studies conducted in this article.

When developing the adaptive system presented in the article, the experience of creating similar systems was taken into account [9]-[11]. At the same time, its distinctive features are optimization of power consumption by the system while maintaining the required accuracy. The analysis of theoretical and applied works in the field of underwater instrumentation has shown that very little attention has been paid to the problem of constructing DAUV control systems optimal by the criterion of energy consumption. This fact can be explained by the idea that mainly water jet and water screw propellers were used as executing mechanisms (EMs) controlling the spatial movement of underwater vehicles. These mechanisms are not able to eliminate the residual buoyancy of the devices, which is the main reason for the increase in energy consumption since the system has to constantly compensate for this buoyancy due to the traction vertical forces of the propeller-type actuator.

To maintain the DAUV at a designated depth, a proportional-integral-derivative (PID) controller and its variations were employed in [12]-[14]. This approach is commonly used in object control due to its simple principle, good adaptability, and ease of implementation [15], [16]. However, attaining precise control of the DAUV in conditions of sea disturbances is quite difficult.

The system being developed for bringing the DAUV to a given depth and stabilizing it at this depth is based on the principle of controlling the residual buoyancy of the DAUV. Papers [17]-[19] present an AUV (Guanay II) which applies a variable buoyancy system for periodic dives, built on the basis of a piston-type pump. The Guanay II is designed for shallow depths, within 40 m, and does not have an outboard pressure compensation system. Besides, the work does not include the buoyancy control system itself. For deep-sea DAUVs operating on the principle of changing the residual buoyancy, a ballast chamber and a pump for pumping and injecting water are required. A low-power DC electric motor (DCM) using battery energy is best suited for controlling such a pump. To reduce the load on the water (hydraulic) pump, it is necessary to apply an external pressure compensation system in the ballast chamber using high-pressure cylinders [20]. Under these conditions, the goal of optimization is to minimize energy consumption.

A distinctive feature of the applied pressure compensation system compared to the one described in article [20] is that the pressure in the ballast chamber is maintained within a specific range. This range is determined by the double amplitude of fluctuations in the stabilization depth of the DAUV. Therefore, the compensation system should not operate when the DAUV is in stabilization mode at a given depth.

2. METHOD

In this work, a DAUV with mass-dimensional and hydrodynamic characteristics was taken as a basis: weight=1,000 kg, length=5,485 mm, diameter=534 mm, shell compression ratio $k_C=0.1$ kg/s², the boundary velocity that determines the DAUV fluid flow mode $v_B=0.2-0.1$ m/s. Factors depending on the shape of the vehicle and the flow regime, which is described by the Reynolds number, are equal to $k_L=40$ kg/s and $k_T=100$ kg, respectively. The shell is located (oriented) vertically. The electric motor of the DI-180 water pump: power $W_{EM}=180$ W, rated voltage $V_N=27$ V, rated operating current $I_N=5$ A. A block of lithium-ion (Li-ion) batteries with a capacity of $C=80$ Ah. Thus, the hydrodynamics of DAUV movement at depth is generally described by (1).

$$\begin{cases} M \frac{d^2h}{dt^2} + k_T \left| \frac{dh}{dt} \right| \cdot \frac{dh}{dt} - k_C h = q(t) + q_0, \text{ if } \frac{dh}{dt} > v_B, \\ M \frac{d^2h}{dt^2} + k_L \cdot \frac{dh}{dt} - k_C h = q(t) + q_0, \text{ if } \frac{dh}{dt} < v_B; \end{cases} \quad (1)$$

where:

- M is the mass of the device, taking into account the attached masses;
- $\frac{d^2h}{dt^2}$, $\frac{dh}{dt}$ is acceleration and speed of vertical movement of the DAUV;
- h is the diving depth of the DAUV;
- $q(t)$ is the change in buoyancy under the influence of a power control action, q_0 is the initial residual buoyancy;
- $q_0(t)$ is the initial buoyancy of the DAUV.

When developing a DAUV diving depth control system, the following factors must be taken into account: the nonlinear dependence of the hydrodynamic drag force on the speed of the DAUV, as well as the non-stationary change in the parameters k_L , k_T and M . It is obvious that direct measurement of these factors in real conditions is impossible, but there are indirect identification methods by which it is possible to obtain estimates of these factors as close as possible to their real values. The information obtained in this way can be used to optimize the DAUV depth management process based on one of the adaptive control methods.

Thus, the objectives that need to be addressed in this work can be identified as follows:

- To determine the structure and principles of the DAUV diving depth management system;
- Develop an algorithm for identifying the factors of M and k_L ;
- To model and analyse the developed system using the MATLAB application software package.

2.1. Development of a block diagram of the drifting autonomous underwater vehicle control system

The DAUV diving depth control system includes two subsystems: a subsystem for bringing the device to a given diving depth and a subsystem for stabilizing the device at this depth. The first equation of the system (1) corresponds to the turbulent mode of fluid flow around the body of the vehicle, specific to the stage of bringing the DAUV to a given depth. The second equation defines the laminar flow mode, which corresponds to the device stabilization period at a given depth or a steady process.

Certain requirements are imposed on the process of bringing the DAUV to a given depth: minimum overshoot and minimum duration. An increase in the astatism of the system leads to an increase in the oscillation of the transition process, and a decrease leads to an increase in the duration. To obtain a compromise option, it is advisable to use a variable structure of the control system. The quality of the established process in the system is determined by the accuracy of determining the parameters of the corrective links. The accuracy of setting these parameters depends on the accuracy of determining the factors M and k_L . To determine these factors, it is proposed to use the compensation type principle of self-adjustment [9], [17].

Figure 1 shows a block diagram of the DAUV control system based on the principle of adaptive control with a self-adjusting model of M_{CO} . Here, the control object (CO) is the hydrodynamic model of the DAUV. The SD depth setter unit generates a signal of the set depth value h_H , which can be either a constant or a variable value, i.e., software-controlled.

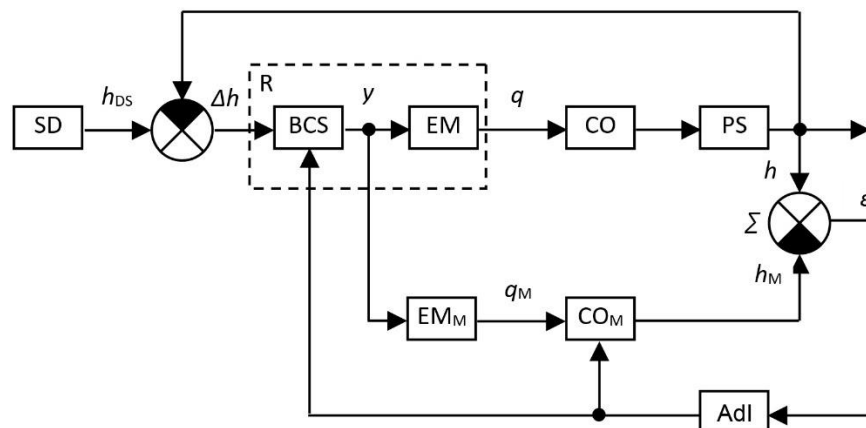


Figure 1. Layout of the adaptive diving depth control system compensation type DAUV with parallel model

The mismatch signal Δh between the set depth value h_{SD} and the current value h is fed to the board control system (BCS), the output control signal y of which is sent to the EM. BCS and EM form the regulating device R of the control system. The EM unit includes a water pump with a DC motor (DCM) and a ballast chamber. The output signal q of the EM block represents a change in the buoyancy of the underwater vehicle and is an argument of the current depth function h , which is measured by the pressure (depth) sensor PS. In parallel with the EM and CO blocks, the model of the EM_M and the model of the CO_M are included. The output signal from the CO_M block in the form of an estimate of the depth h_M is compared on the adder Σ with the signal h . The difference ε of these signals is received at the input of the adaptive identification (AdI) unit. An optimization criterion of the form is formed in the AdI unit (2):

$$J = f[\varepsilon(t)] \quad (2)$$

The value of the quality criterion serves as a measure of approximation of the CO and its model parameters. Next, the output signal of the AdI unit continuously adjusts the parameters of CO_M , in order to minimize the optimization criterion, and simultaneously changes the parameters of the correction algorithm synchronously in the BCS unit. The most common forms of implementation of the AdI principles currently include methods that can be combined under a common name – gradient methods [21].

2.2. Mathematical modeling of the drifting autonomous underwater vehicle control system

Figure 2 shows the structure of the control object CO. It provides a schematic representation of the system in (1). The CO includes sequentially connected inertial and integrating links covered by positive feedback (k_C).

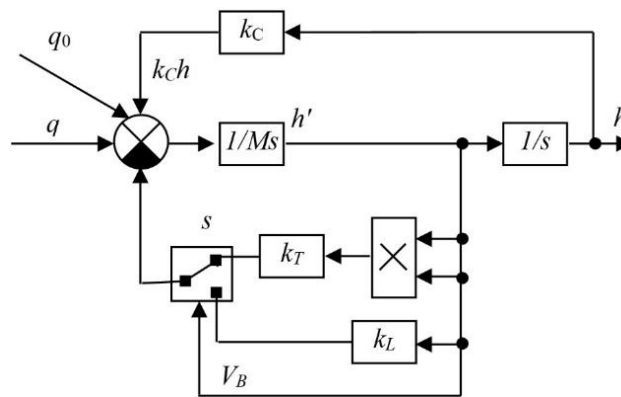


Figure 2. Block diagram of the CO

The diagram has a variable structure, i.e., the movement of the DAUV obeys the first equation of the system in the mode of bringing the DAUV to a given depth at a speed less than the boundary (1). When the speed reaches the boundary value v_B , the driving mode is switched (switch s) to the second equation. In this case, the equation system can be replaced by a transfer function that describes the movement of the DAUV in the steady-state stabilization mode.

$$W_{CO} = \frac{1}{Ms^2 + k_L s - k_C}. \quad (3)$$

The EM (Figure 1) consists of sequentially connected integrating and inertial links and includes a DCM, a water pump and a ballast chamber. The transfer function of EM has the following form (4).

$$W_{EM} = \frac{1}{s(Ts+1)}. \quad (4)$$

The EM is controlled by the BCS. Figure 3 shows the general structure of the BCS algorithm. Although the control law is implemented on a software basis in a real system, it can be presented structurally for clarity. Conventionally, the system (Figure 3) can be divided into two subsystems. This is a PID controller (proportional-integral-differentiating link) and a relay unit (RU) (RU includes a bipolar contactless relay link relay element (RE) with a dead zone and hysteresis, covered by a reverse negative integrating link).

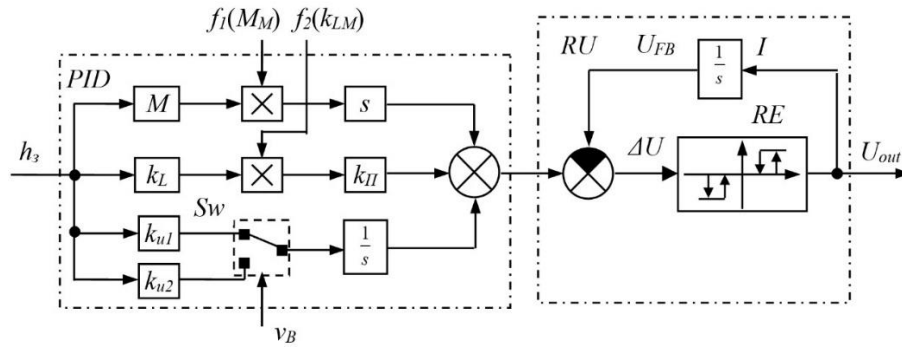


Figure 3. Diagram of a BCS with a variable structure

The main purpose of the gain factors of the differentiating and proportional links is to compensate for the influence of non-stationary and nonlinear parameters M and k_L on the quality of the steady-state CO process. In this regard, the structure of the PID controller provides for the possibility of adjusting these parameters using the AdI unit (Figure 1). Besides, to reduce the oscillation of the transient process, a switch of the astatic link gain (Sw) is included in the PID controller circuit, which is triggered when the DAUV immersion rate decreases below v_B .

The relay unit is designed to control the operation of the water pump. The integrator (I) in the negative feedback circuit of the RE gives the system qualitatively new properties, creating a relay-pulse mode of operation or pulse-width modulation of the input effect. Figure 4 shows the static properties of RE.

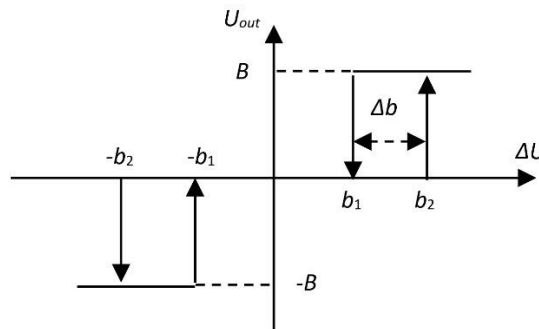


Figure 4. Graphic properties of the RE

The period of the control pulses at the output of the RE is determined by (5):

$$T = t_1 + t_2 = \frac{\Delta b}{\dot{U}_{in}} + \frac{\Delta b}{\dot{U}_{fb} - \dot{U}_{in}}, \tag{5}$$

here t_1 is the section where $U_{out}=0$, and t_2 is the section that corresponds to $U_{out}=B$.

Thus, taking into account (5), it is possible to write down the average value of the output signal for the pulse repetition period.

$$U_{out.av} = \frac{Bt_2}{t_1+t_2} = \frac{B}{\frac{t_1}{t_2}+1} = \frac{B \cdot \dot{U}_{in}}{\dot{U}_{fb}}. \tag{6}$$

When the dead zone Δb tends to zero, it can be assumed that the instantaneous value of the output signal is equal to the average, i.e., $U_{out} = U_{out.av}$, and expression (6) can be represented as (7).

$$U_{out} = \frac{B \cdot \dot{U}_{in}}{\dot{U}_{fb}}. \tag{7}$$

As a result, the relay link covered by the integrating feedback can, in the first approximation, be replaced by two sequentially connected links: an amplifying link with a dead zone and a differentiating link. Thus, when the hysteresis of the RE tends to zero, a so-called sliding mode occurs [22], and the structure in Figure 4 can be represented in an equivalent form (Figure 5). Here the RE is replaced by a nonlinear element of the backlash type (NE), and a differentiating link (DL) is installed in the direct circuit (Figure 5) instead of the integrator (I) in the feedback circuit (Figure 3). Thus, the astatism introduced by DCM as an integrating link is eliminated, and a DCM control mode is created, which belongs to the category of the most economical control modes of low-power DCM. A prerequisite for such a relay control method lies in self-oscillations in the system output signal, i.e., the h signal. In this case, the amplitude of the output self-oscillating process is directly proportional to the dead zone of the RE or the backlash of the nonlinear element NE.

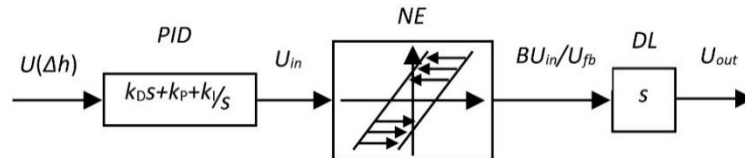


Figure 5. Equivalent diagram of the basic BSU control law

2.3. Identification of hydrodynamic parameters of the drifting autonomous underwater vehicle

As it was determined above, it is advisable to use one of the gradient methods to identify the DAUV parameters. The general form of the organization of the movement to the extremum by gradient methods is reduced to such a change in the vector of parameters $\mathbf{A} = (a_1, a_2, \dots, a_n)^T$, at which its rate of change is related to the gradient of the function J by the ratio:

$$d\mathbf{A}/dt = \mathbf{B}(\mathbf{A}) \text{grad}_A J(\mathbf{A}), \quad (8)$$

where \mathbf{B} is some square n -matrix with elements depending in the general case on \mathbf{A} , $\text{grad}_A J(\mathbf{A}) = (\frac{\partial J}{\partial a_1}, \frac{\partial J}{\partial a_2}, \dots, \frac{\partial J}{\partial a_n})^T$ is a vector column of partial derivatives J by a_i . In this case, $n=2$, $a_1=M$, $a_2=k_L$ and $\text{grad}_A J(\mathbf{A}) = (\frac{\partial J}{\partial M}, \frac{\partial J}{\partial k_L})^T$. One or another algorithm of movement to the extreme is formed depending on the specific type of matrix \mathbf{B} . One of the most common methods of reaching the extremum is the method of auxiliary operator (MAO) [6].

2.3.1. Method of auxiliary operator

The MAO refers to non-search compensation methods for identifying unknown parameters, where a self-adjusting model is used (Figure 6) with parameter adjustment according to the gradient of the functional mismatch of the outputs of the object ($W_{CO}(s, a_i)$) and models ($W_M(s, a_i)$) with a common input signal and an auxiliary operator ($W_A(s, a_i)$) to obtain partial derivatives $\frac{\partial J}{\partial a_i}$ by configurable parameters from the mismatch signal of the object and the model using the multiplication unit MU. For qualitative parametric identification, it is necessary that the input signal q includes regular interference or an artificial harmonic signal [23], [24]. In this case, the role of such an auxiliary signal is performed by self-oscillations caused by the relay unit RU (Figure 2). The mismatch of the outputs of the object and the model is denoted as an error (ε) (8) when using this method takes looks as (9):

$$d\mathbf{A}/dt = \mathbf{\Gamma} \text{grad}_A J(\varepsilon), \quad (9)$$

where $\mathbf{\Gamma} = \text{diag} \{ \gamma_1, \gamma_2, \dots, \gamma_n \}$ is a diagonal matrix of constant factors (gain factors) in the self-adjustment loop. Components of the gradient of the functional $J(\varepsilon)$ are determined by the usual differentiation rule of a complex function $J(\varepsilon)$ by the argument a_i ($i=1, 2, \dots, n$).

$$\frac{\partial J}{\partial a_i} = \frac{\partial J(\varepsilon)}{\partial \varepsilon} \cdot \frac{\partial \varepsilon}{\partial a_i}. \quad (10)$$

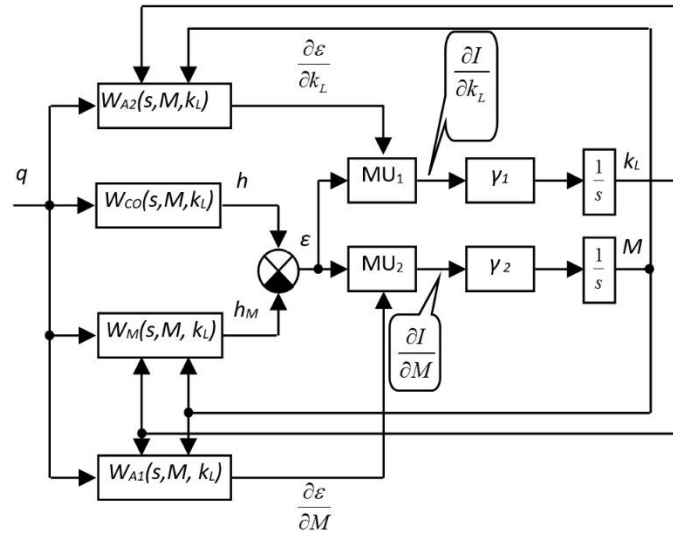


Figure 6. Block diagram of parameter identification

Optimization criterion (2) can be presented as (11):

$$J = \frac{1}{2} \varepsilon^{-2} \tag{11}$$

a 1/2 multiplier has been added here for the convenience of further transformations, and the dash symbolically denotes the averaging operation over time. From (10), taking into account (11), will be as (12).

$$\frac{\partial J}{\partial a_i} = \varepsilon \cdot \frac{\partial \varepsilon}{\partial a_i} \tag{12}$$

The gradient algorithm for setting the parameters a_i based on the condition of achieving the minimum of the functional $J(\varepsilon)$ can be represented in the following scalar form (13):

$$\frac{da_i}{dt} = -\gamma_i \varepsilon \frac{\partial \varepsilon}{\partial a_i} \text{ or } s a_i = -\gamma_i \varepsilon \frac{\partial \varepsilon}{\partial a_i}, \tag{13}$$

where $s = \frac{d}{dt}$ is the differentiation operator.

In other words, the movement to the optimal value of J goes along the gradient towards its optimal value at a speed proportional to the gradient of J . The multiplier $\frac{\partial \varepsilon}{\partial a_i}$ is determined from (13):

$$\frac{\partial \varepsilon}{\partial a_i} = \frac{\partial}{\partial a_i} (h_0 - h_M) = -\frac{\partial h_M}{\partial a_i} = -\frac{\partial [W_M(s, a_i) q]}{\partial a_i} = -\frac{\partial [W_M(s, a_i) q]}{\partial a_i} = -\frac{q \partial W_M(s, a_i)}{\partial a_i} - W_M(s, a_i) \frac{\partial q}{\partial a_i}, \tag{14}$$

since $\frac{\partial q}{\partial a_i} = 0$, then (14) can be simplified as (15):

$$\frac{\partial \varepsilon}{\partial a_i} = -\frac{q \partial W_M(s, a_i)}{\partial a_i} = q W_{Bi}(s, a_i), \frac{\partial \varepsilon}{\partial a_i} = -\frac{q \partial W_M(s, a_i)}{\partial a_i} = q W_{Bi}(s, a_i), \tag{15}$$

where $W_{Ai} = -\frac{\partial W_M(s, a_i)}{\partial a_i}$ is the auxiliary operator.

In this case, the number of variable parameters is 2, i.e., $i=2$, $\Gamma = \text{diag} \{ \gamma_1, \gamma_2 \}$, $\mathbf{A} = \{ a_1, a_2 \}$, $a_1 = M$ and $a_2 = k_L$. In relation to the system being developed, auxiliary operators take (16).

$$W_{A1}(s, M) = \left(\frac{1}{Ms^2 + k_L s - k_C} \right)'_M = \frac{s^2}{(Ms^2 + k_L s - k_C)^2}, \tag{16}$$

$$W_{A2}(s, k_L) = \left(\frac{1}{Ms^2 + k_L s - k_C} \right)'_{k_L} = \frac{s}{(Ms^2 + k_L s - k_C)^2}.$$

The described algorithm for identifying parameters can be presented in the form of a block diagram as shown in Figure 6. In this case, the transfer function of the CO model $W_M(s, M, k_L)$ is advisable to present as (17).

$$W_M(s, M, k_L) = \frac{1}{\left(\frac{M}{k_L}s+1\right)k_L+k_C}. \tag{17}$$

The structure corresponding to this type of transfer function is shown in Figure 7. The block diagram of transfer function $W_M(s, M, k_L)$ is provided for clarity. The block diagram of transfer function W is provided for clarity. The division blocks DB1 and DB2 receive the output signals of the identification unit AdI (Figure 1).

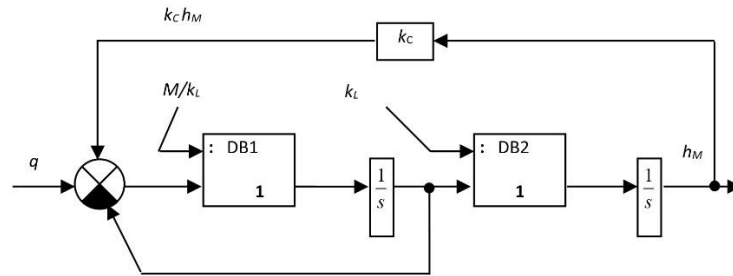


Figure 7. Block diagram of transfer function $W_M(s, M, k_L)$

2.3.2. Modified method of auxiliary operator

In many practical problems, the algorithm known as the generalized Newton method is recognized as one of the most successful in terms of the speed of reaching the extremum when searching for the extremum of multidimensional functions [25]. The combined use of MAO techniques and the generalized Newton method can be given a conditional name – the modified method of auxiliary operator (MMAO). This method follows from the general relation (9) if the negative inverse matrix of the second derivatives (Hesse or Hessian matrix) of the function J in A is used as the matrix B , i.e.,

$$B(A) = - \left[\frac{d^2}{dA^2} J(\epsilon) \right]^{-1}. \tag{18}$$

Thus, the algorithm of movement to the extremum by the generalized Newton method takes the form (19).

$$\frac{dA}{dt} = - \left[\frac{d^2}{dA^2} J(\epsilon) \right]^{-1} \text{grad}_A J(\epsilon). \tag{19}$$

If we turn again to a specific control system, i.e., $A=\{M, k_L\}$, we can write:

$$\frac{dA}{dt} = - \begin{vmatrix} \frac{\partial^2 J}{\partial k_L^2} \frac{1}{\Delta} & -\frac{\partial^2 J}{\partial k_L \partial M} \frac{1}{\Delta} \\ -\frac{\partial^2 J}{\partial M \partial k_L} \frac{1}{\Delta} & \frac{\partial^2 J}{\partial M^2} \frac{1}{\Delta} \end{vmatrix} \times \begin{vmatrix} \frac{\partial J}{\partial M} \\ \frac{\partial J}{\partial k_L} \end{vmatrix}, \tag{20}$$

here $\text{grad}_A J(\epsilon) = \begin{vmatrix} \frac{\partial J}{\partial M} \\ \frac{\partial J}{\partial k_L} \end{vmatrix}$; $\frac{d^2}{dA^2} J(\epsilon) = \begin{vmatrix} \frac{\partial^2 J}{\partial M^2} & \frac{\partial^2 J}{\partial M \partial k_L} \\ \frac{\partial^2 J}{\partial k_L \partial M} & \frac{\partial^2 J}{\partial k_L^2} \end{vmatrix}$;

$$\left[\frac{d^2}{dA^2} J(\epsilon) \right]^{-1} = \begin{vmatrix} \frac{\partial^2 J}{\partial M^2} \frac{1}{\Delta} & \frac{\partial^2 J}{\partial M \partial k_L} \frac{1}{\Delta} \\ \frac{\partial^2 J}{\partial k_L \partial M} \frac{1}{\Delta} & \frac{\partial^2 J}{\partial k_L^2} \frac{1}{\Delta} \end{vmatrix}; \tag{21}$$

where $\Delta = \frac{\partial^2 J}{\partial M^2} \frac{\partial^2 J}{\partial k_L^2} - \frac{\partial^2 J}{\partial M \partial k_L} \frac{\partial^2 J}{\partial k_L \partial M} = \frac{\partial^2 J}{\partial M^2} \frac{\partial^2 J}{\partial k_L^2} - \left(\frac{\partial^2 J}{\partial M \partial k_L}\right)^2$ is the $\frac{d^2}{dA^2} J(\epsilon)$ matrix determinant

$$\begin{aligned} \frac{\partial J}{\partial M} &= \varepsilon \frac{\partial \varepsilon}{\partial M} = \varepsilon \frac{\partial y_M}{\partial M} = \varepsilon \left(\frac{q}{Ms^2+k_Ls-k_C} \right)'_M = -\varepsilon \frac{qs^2}{(Ms^2+k_Ls-k_C)^2}; \\ \frac{\partial J}{\partial k_L} &= \varepsilon \frac{\partial \varepsilon}{\partial k_L} = \varepsilon \left(\frac{q}{Ms^2+k_Ls-k_C} \right)'_{k_L} = -\varepsilon \frac{qs}{(Ms^2+k_Ls-k_C)^2}; \\ \frac{\partial^2 J}{\partial M^2} &= \left(\varepsilon \frac{\partial \varepsilon}{\partial M} \right)'_M = \left(\frac{\partial \varepsilon}{\partial M} \right)^2 + \varepsilon \left(\frac{\partial^2 \varepsilon}{\partial M^2} \right); \\ \frac{\partial^2 J}{\partial k_L^2} &= \left(\varepsilon \frac{\partial \varepsilon}{\partial k_L} \right)'_{k_L} = \left(\frac{\partial \varepsilon}{\partial k_L} \right)^2 + \varepsilon \left(\frac{\partial^2 \varepsilon}{\partial k_L^2} \right); \end{aligned}$$

here

$$\begin{aligned} \frac{\partial^2 \varepsilon}{\partial M^2} &= \frac{q \cdot 2s^4}{(Ms^2+k_Ls-k_C)^3} \text{ and } \frac{\partial^2 \varepsilon}{\partial k_L^2} = \frac{q \cdot 2s^2}{(Ms^2+k_Ls-k_C)^3}; \\ \frac{\partial^2 J}{\partial M \partial k_L} &= \frac{\partial^2 J}{\partial M \partial k_L} = \left(\varepsilon \frac{\partial \varepsilon}{\partial M} \right)'_{k_L} = \frac{\partial \varepsilon}{\partial k_L} \frac{\partial \varepsilon}{\partial M} + \varepsilon \frac{\partial^2 \varepsilon}{\partial M \partial k_L}; \\ \frac{\partial^2 \varepsilon}{\partial M \partial k_L} &= \left[-\frac{qs}{(Ms^2+k_Ls-k_C)^2} \right]'_M = \frac{q \cdot 2s^3}{(Ms^2+k_Ls-k_C)^3}. \end{aligned}$$

As a result, the vector $\frac{dA}{dt}$ can be represented by a system of (22).

$$\begin{cases} \frac{dM}{dt} = -\frac{1}{\Delta} \left(\frac{\partial J}{\partial M} \frac{\partial^2 J}{\partial k_L^2} - \frac{\partial J}{\partial k_L} \frac{\partial^2 J}{\partial M \partial k_L} \right) \\ \frac{dk_L}{dt} = -\frac{1}{\Delta} \left(\frac{\partial J}{\partial M} \frac{\partial^2 J}{\partial k_L \partial M} + \frac{\partial J}{\partial k_L} \frac{\partial^2 J}{\partial M^2} \right) \end{cases} \quad (22)$$

Substituting its value instead of the determinant Δ , we get (23):

$$\begin{cases} \frac{dM}{dt} = -\frac{\frac{\partial J}{\partial M} \frac{\partial^2 J}{\partial k_L^2} - \frac{\partial J}{\partial k_L} \frac{\partial^2 J}{\partial M \partial k_L}}{\frac{\partial^2 J}{\partial M^2} \frac{\partial^2 J}{\partial k_L^2} - \left(\frac{\partial^2 J}{\partial M \partial k_L} \right)^2} \\ \frac{dk_L}{dt} = -\frac{\frac{\partial J}{\partial k_L} \frac{\partial^2 J}{\partial M^2} - \frac{\partial J}{\partial M} \frac{\partial^2 J}{\partial M \partial k_L}}{\frac{\partial^2 J}{\partial M^2} \frac{\partial^2 J}{\partial k_L^2} - \left(\frac{\partial^2 J}{\partial M \partial k_L} \right)^2} \end{cases} \quad (23)$$

The first of the considered algorithms (16), when searching for an extremum, is characterized by a fairly stable process of searching for such a value of vector **A**, which corresponds to the extreme value of the functional *J*. However, the convergence rate of the search is low. The second algorithm (23), on the contrary, is recognized as the most successful in terms of the speed of reaching the extremum. For qualitative and quantitative evaluation of these two algorithms, it is necessary to conduct a comparative computer simulation of the DAUV diving depth control system, taking into account the specific weight, size, and hydrodynamic properties of the underwater vehicle and the technical parameters of individual system components (1).

3. RESULTS AND DISCUSSION

A model of the DAUV diving depth control system with a non-stationary parameters identification block (PIB) in the Simulink environment was developed (Figure 8) based on the block diagram (Figure 1). The whole diagram can be divided into three subsystems. Subsystem 1 is a CO. Subsystem 2 is a process regulator R and includes a BCS and an EM. Subsystem 3 or the parametric identification block (PIB) consists of a set of BCS models and a CO (BCS_M+CO_M), a block of auxiliary operators (BAO), a block of multiplication (BMP) and other elements that ensure the identification process. The structural diagrams of Figures 3, 6, and 7 became the basis for the construction of individual subsystems of the obtained Simulink model.

Simulink-model of the CO (Figure 9) implements the system of (1) and provides a transition from the turbulent flow around the shell of the vehicle to the laminar flow with a decrease in the diving rate of the DAUV below *V_B*. The Simulink CO model was developed in accordance with the structural diagram (Figure 2). The Simulink model of the BCS is built in accordance with the structural diagram (Figure 3) and includes a PID link with a variable structure and a relay unit RU (Figure 10).

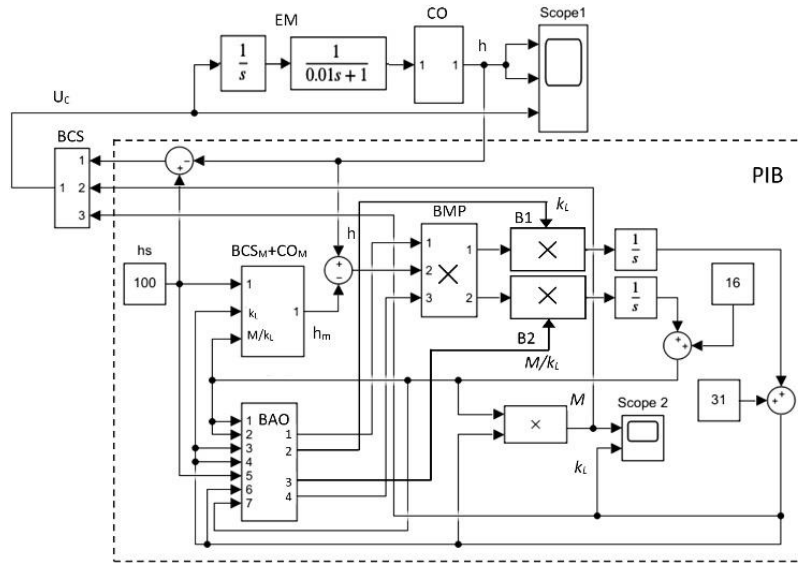


Figure 8. Simulink-model of the DAUV diving depth control system with non-stationary parameter identification

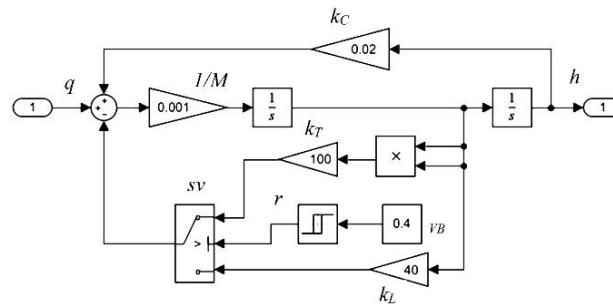


Figure 9. Simulink CO model

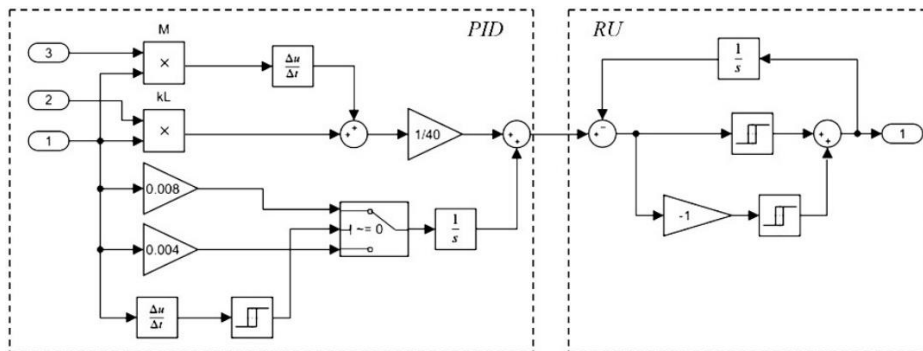


Figure 10. Simulink-model of the BCS

The EM consists of sequentially connected links: an integrating link and an inertial one (Figure 8). The Simulink model of the CO was developed in accordance with the structural diagram (Figure 2) and is presented in Figure 9. The BCS is shown in Figure 10.

The Simulink model of BCS_M completely duplicates the Simulink model of BCS. The CO_M Simulink model is shown in Figure 11. The structure in Figure 11 differs from the Simulink model of the CO by additional inputs, with the help of which the factors *M* and *k* are adjusted. It is advisable to present the model of the transfer function of the CO_M in a two-circuit form, where proportional links with variable factors are

replaced by division blocks since it is impossible to directly change the parameters of the links during modelling in the MATLAB system. At the same time, the initial (predicted) values of these factors seen in Figure 8 are respectively equal to $M/16=496/16=31$ and $k_L=16$.

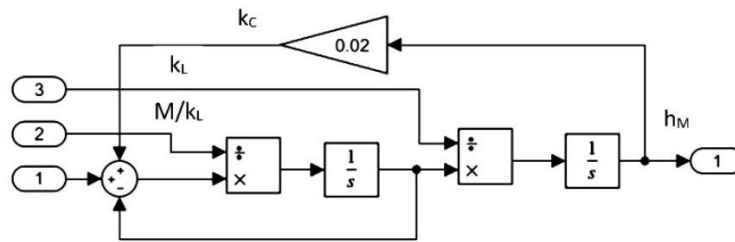


Figure 11. Simulink-model of CO_M

The BMP implements (13); constant factors γ_1 and γ_2 are used as matrices B_1 and B_2 when applying the auxiliary factors. When using the modified method of auxiliary coefficients, the following ratios (21) are applied. Figures 12 and 13 show the results of modelling the process using the Simulink model shown in Figure 8. Figure 12 shows results of bringing the DAUV to a given diving depth (for clarity, $h_s=100$ m is assumed) using MAO techniques in Figure 12(a) and the processes of identifying the parameters M and k_L in Figure 12(b).

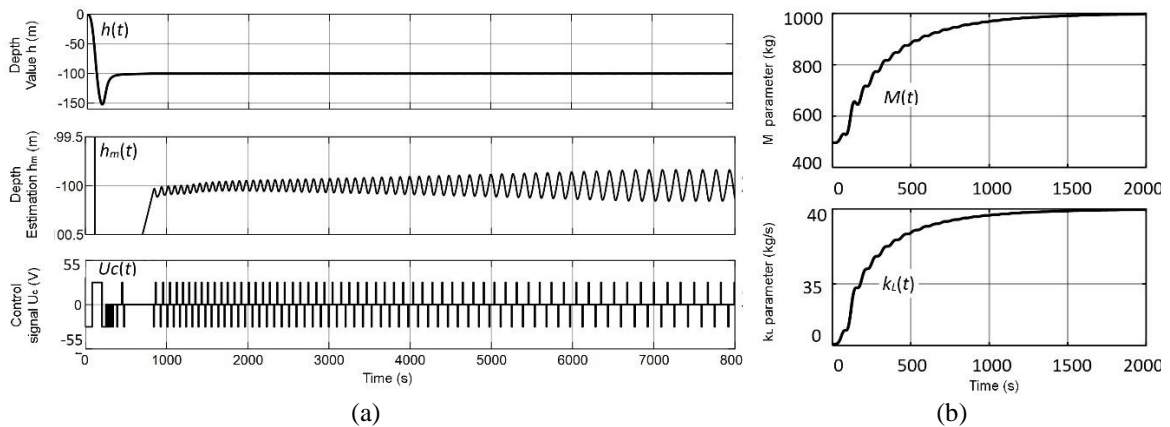


Figure 12. Simulation results in the DAUV control system using MAO techniques; (a) transients processes and (b) the process of identifying M and k_L parameters

Figure 13 shows results of stabilizing the DAUV at 100 m depth using MMAO techniques in Figure 13(a), as well as the processes of identifying the parameters M and k_L in Figure 13(b). In Figure 12 and Figure 13, the following designations are adopted: $h(t)$ is the current depth of the DAUV, $h_m(t)$ —graph $h(t)$ on an enlarged scale, $U_c(t)$ —control signals coming to the DC motor of the water pump, $M(t)$ and $k_L(t)$ the output signals of the identification block are the correction parameters M and k_L . Parameters of the steady-state self-oscillating process: self-oscillation period $T=160$ s; amplitude $A \leq 0.5$ m.

A comparative analysis of the waveforms in Figure 12(a) and Figure 13(a) shows that the transient process of self-oscillation stabilization caused by the adjustment of the parameters M and k_L in the second case, ends at around 500 s, and in the first case – at around 700 s. The waveforms (Figure 12(b) and Figure 13(b)) confirm that the duration of the transition process when using the generalized Newton method (Figure 13(b)) is reduced by about two times compared with using the MAO method.

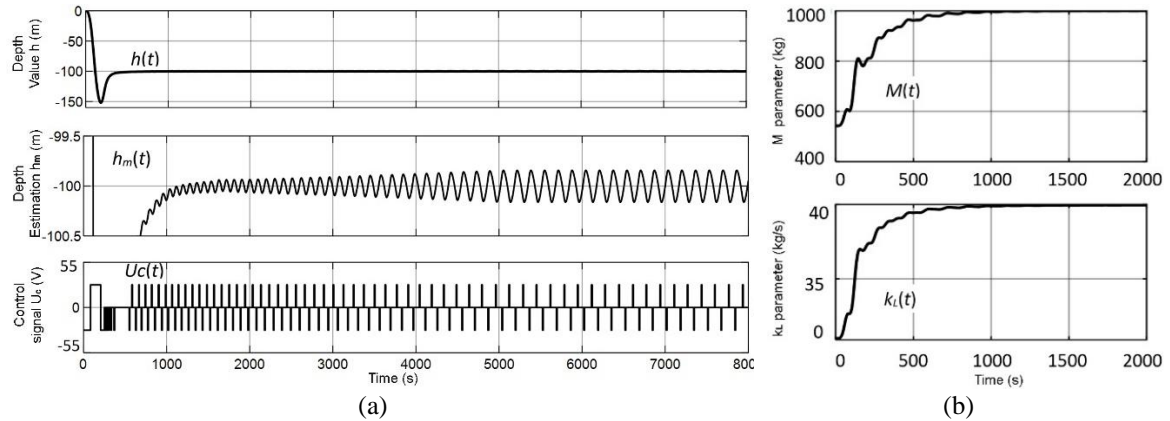


Figure 13. Simulation results in the DAUV control system with MMAO techniques; (a) transients processes and (b) the process of identifying M and k_L parameters

For comparison, Figure 14 shows similar waveforms obtained for the DAUV control system with M and k_L parameters correction disabled. In this case, the gain of the astatic link is constant. Visual analysis shows that the amplitude of self-oscillations $h(t)$ in this system significantly exceeds the amplitude of self-oscillations $h(t)$ in Figures 12 and 13.

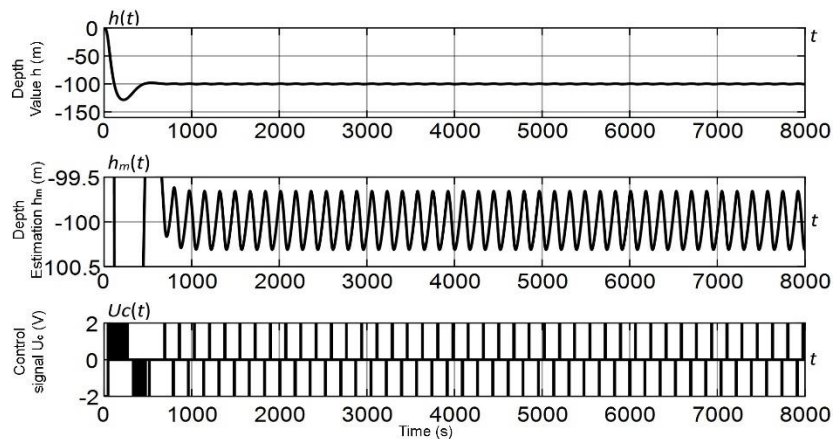


Figure 14. Simulation results in the DAUV control system with disabled correction of M and k_L parameters and a constant gain of the astatic link

The battery life of the DAUV (T_A) depends on the energy consumption of the electric motor and the duty cycle of the power control pulses (Q_{IM}). We can write $T_A = Q_{IM} * C / I_N$. By increasing the time scale of the obtained waveforms (Figures 12 and 13), it is possible to measure the width of the pulses $U_C(t)$ and calculate the intermittency factor. As a result, the calculated value of $T_A = 1920 \text{ hours} = 80 \text{ days}$. For the system shown in Figure 14, $T_A = 40 \text{ days}$. Significant reduction of the pulse duty cycle $U_C(t)$ (Figure 14) is explained by an increase in the width of the control pulses, which also explains the increase in the amplitude of self-oscillations. Thus, it is possible to draw a preliminary conclusion about the feasibility of using a control system with a variable structure and technology for non-stationary identifying hydrodynamic parameters of the DAUV to create a working sample of the DAUV.

4. CONCLUSION

This paper proposed the structure of an adaptive diving depth control system for an autonomous underwater vehicle, based on the identification of non-stationary parameters of the DAUV as a CO. Mathematical and computer models of identification algorithms were presented during the study. Two identification algorithms were taken as a basis: an algorithm based on the method of auxiliary factors and an

algorithm based on a modified generalized Newton method. A computer simulation was developed using the Simulink package and the MATLAB environment. The mass-dimensional parameters of the DAUV, specific to small-sized underwater vehicles, were used during the calculations. The obtained Simulink models did not show the mechanism for adjusting the parameters of the DAUV diving depth control algorithm itself, since the study of the operation modes of the adaptive DAUV diving depth control system and control optimization is a topic of future independent research. The objective of this study was to substantiate the possibility of obtaining reliable information on the non-stationary parameters of the DAUV as a hydrodynamic object, to consider alternative methods for finding the minimum of the two-dimensional function $J[\varepsilon(M, k_L)]$ and to choose the most appropriate method to ensure quality control. The main criterion for choosing the best method was the stability of the identification process and its speed. As can be derived from the computer simulation, the proposed modified generalized Newton's method has shown the best results according to these criteria and can be recommended for application in subsequent studies.

ACKNOWLEDGEMENTS

This research was funded by the Ministry of Science and Higher Education of the Republic of Kazakhstan (Grant No. AP13268732).

REFERENCES




- [1] H. Xiao, R. Cui and D. Xu, "A sampling-based Bayesian approach for cooperative multiagent online search with resource constraints," *IEEE Transactions on Cybernetics*, vol. 48, no. 6, pp. 1773-1785, Jun. 2018, doi:10.1109/TCYB.2017.2715228.
- [2] Y. Yang, Y. Xiao, and T. Li, "A Survey of autonomous underwater vehicle formation: performance, formation control, and communication capability," in *IEEE Communications Surveys & Tutorials*, vol. 23, no. 2, pp. 815-841, 2021, doi: 10.1109/COMST.2021.3059998.
- [3] A. Wibisono, M. J. Piran, H.-K. Song, and B. M. Lee, "A survey on unmanned underwater vehicles: challenges, enabling technologies, and future research directions," *Sensors*, vol. 23, no. 17, 2023, doi: 10.3390/s23177321.
- [4] M. W. Hasan, and N. H. Abbas, "An improved swarm intelligence algorithms-based nonlinear fractional order-PID controller for a trajectory tracking of underwater vehicles," *TELKOMNIKA Telecommunication, Computing, Electronics and Control*, vol. 18, no. 6, pp. 3173-3183, Dec. 2020, doi: 10.12928/TELKOMNIKA.v18i6.16282.
- [5] E. N. Pantov, N. N. Makhin, and B. B. Sheremetov, "Fundamentals of the Theory of Motion of Underwater Vehicles," *Leningrad: Sudostroenie*, 1973 [in Russian].
- [6] S. Wadoo, and P. Kachroo, *Autonomous underwater vehicles: modeling control design and simulation*, Boca Raton: CRC Press, 2011.
- [7] T. Braunl, A. Boeing, L. Gonzalez, A. Koestler, and M. Nguyen, "Design, modelling and simulation of an autonomous underwater vehicle," *Int. J. of Vehicle Autonomous Systems*, vol. 4, no. 2-4, pp. 106-121, 2006, doi: 10.1504/IJVAS.2006.012202.
- [8] A. V. Inzartsev *et al.*, "The integrated navigation system of an autonomous underwater vehicle and the experience from its application in high Arctic latitudes," *Gyroscopy and Navigation*, vol. 1, no. 2, pp. 107-112, 2010, doi: 10.1134/S2075108710020045.
- [9] C. McGann, F. Py, K. Rajan, J. Ryan, and R. Henthorn, "Adaptive control for autonomous underwater vehicles," in *AAAI'08: Proceedings of the 23rd national conference on Artificial intelligence*, 2008, pp. 1319-1324, doi: 10.5555/1620270.1620279.
- [10] Y. C. Sun and C. C. Cheah, "Adaptive setpoint control for autonomous underwater vehicles," *42nd IEEE International Conference on Decision and Control (IEEE Cat. No.03CH37475)*, Maui, HI, USA, 2003, vol. 2, pp. 1262-1267, doi: 10.1109/CDC.2003.1272782.
- [11] Y. C. Sun and C. C. Cheah, "Adaptive setpoint control of underwater vehicle-manipulator systems," *IEEE Conference on Robotics, Automation and Mechatronics, Singapore*, 2004, vol. 1, pp. 434-439, doi: 10.1109/RAMECH.2004.1438959.
- [12] B. Hu, H. Tian, J. Qian, G. Xie, L. Mo, and S. Zhang, "A fuzzy-PID method to improve the depth control of AUV," *2013 IEEE International Conference on Mechatronics and Automation*, Takamatsu, Japan, 2013, pp. 1528-1533, doi: 10.1109/ICMA.2013.6618141.
- [13] M. S. Ajmal, M. Labeeb, and D. V. Dev, "Fractional order PID controller for depth control of autonomous underwater vehicle using frequency response shaping approach," *2014 Annual International Conference on Emerging Research Areas: Magnetics, Machines and Drives (AICERA/iCMMD)*, Kottayam, India, 2014, pp. 1-6, doi: 10.1109/AICERA.2014.6908219.
- [14] Z. Zhang, B. Liu, and L. Wang, "Autonomous underwater vehicle depth control based on an improved active disturbance rejection controller," *International Journal of Advanced Robotic Systems*, vol. 16, no. 6, 2019, doi:10.1177/1729881419891536.
- [15] H. S. Dakheel, Z. B. Abdullah, N. S. Jasim, and S. W. Shneen, "Simulation model of ANN and PID controller for direct current servo motor by using Matlab/Simulink," *TELKOMNIKA Telecommunication, Computing, Electronics and Control*, vol. 20, no. 4, pp. 922-932, 2022, doi: 10.12928/TELKOMNIKA.v20i4.23248.
- [16] L. Li, J. Xie, and W. Li, "Fuzzy adaptive PID control of a new hydraulic erecting mechanism," *TELKOMNIKA Telecommunication, Computing, Electronics and Control*, vol. 11, no. 4, pp. 715-724, Dec. 2013, doi: 10.12928/TELKOMNIKA.v11i4.1159.
- [17] I. Masmijà, J. González, and S. Gomàriz, "Buoyancy model for Guanay II AUV," *OCEANS 2014 - TAIPEI*, Taipei, Taiwan, 2014, pp. 1-7, doi: 10.1109/OCEANS-TAIPEI.2014.6964545.
- [18] W. A. P. MuñOz, A. G. Sellier, and S. G. Castro, "The predictive functional control and the management of constraints in Guanay II autonomous underwater vehicle actuators," *IEEE Access*, vol. 6, pp. 22353-22367, 2018, doi: 10.1109/ACCESS.2018.2828325.
- [19] C. Galarza, I. Masmijà, J. Prat, and S. Gomàriz, "Design of obstacle detection and avoidance system for Guanay II AUV," *2016 24th Mediterranean Conference on Control and Automation (MED)*, Athens, Greece, 2016, pp. 410-414, doi: 10.1109/MED.2016.7535959.
- [20] Y. Li, and QF Wang, "Research on the pressure compensation for the underwater hydraulic motor," *Underwater Technology: The International Journal of The Society for Underwater*, vol. 26, pp. 89-96, 2005, doi: 10.3723/175605405784426673.
- [21] Y. Nesterov, "Gradient methods for minimizing composite functions," *Mathematical Programming*, vol. 140, pp. 125-161, 2013,

doi: 10.1007/s10107-012-0629-5.




- [22] Ş. K. Yıldız and H. Demircioğlu, "Relay sliding mode control of multiloop systems based on the input-output model," *2015 IEEE Conference on Control Applications (CCA)*, Sydney, NSW, Australia, 2015, pp. 834-839, doi: 10.1109/CCA.2015.7320721.
- [23] N. Kosulina, S. Kosulin, K. Korshunov, T. Nosova, and Y. Nosova, "Determination of hydrodynamic parameters of the sealed pressure extractor", *IAPGOS*, vol. 11, no. 2, pp. 44-47, Jun. 2021, doi: 10.35784/iapgos.2657.
- [24] W. Sun, and Y. Yuan, *Optimization theory and methods. Nonlinear programming*, Springer NY, 2010, doi: 10.1007/b106451.
- [25] V. K. Pillai and H. D. Nelson, "A generalized newton Raphson method for limit cycle analysis of nonlinear control systems," *1987 American Control Conference*, Minneapolis, MN, USA, 1987, pp. 1213-1218, doi: 10.23919/ACC.1987.4789499.

BIOGRAPHIES OF AUTHORS






Viktor Ivel    was born in 1950. He received his engineering degree in automation and telemechanic from the Kazakh Polytechnic Institute in 1974 and his Ph.D. degree from the «HydroPribor» St. Petersburg Research Institute in 1983. In 2002, he obtained his HDR degree in electronics. Now he is a professor and doctoral student supervisor at the North-Kazakhstan University, Petropavlovsk. His research interests include ECG monitoring systems, Holter monitoring, pattern recognition, neural network systems, signal identification, and signal processing. He can be contacted at email: vivel@ku.edu.kz.






Yuliya Gerasimova    was born in 1979. She received her engineering degree in automation and control of technological processes and production facilities from North Kazakhstan University in 2001. In 2010 she received her Ph.D. degree from East Kazakhstan State Technical University, Oskemen, Republic of Kazakhstan. Since 2011, she works as a senior lecturer at the Department of Energetic and Radioelectronics, North-Kazakhstan University, Petropavlovsk. Her research interests include signal recognition, signal processing, ECG monitoring systems, automatic, and control systems. She can be contacted at email: yugerasimova@ku.edu.kz.



Sayat Moldakhmetov    received a bachelor's degree in engineering and technology and a master of technical sciences in the field of radio engineering, electronics and telecommunications at M. Kozybayev North-Kazakhstan University, Petropavlovsk, Kazakhstan, in 2010 and 2012, respectively. In 2013-2016 he studied for a doctorate at Satpayev University, Almaty, Kazakhstan. In 2021, he defended his dissertation on the topic "Research on methods for switching voltage stages of a multi-level power inverter." Currently he is an associate professor of the Department of Energy and Radioelectronics at the M. Kozybayev North-Kazakhstan University. He is also the leader of the project AP13268732 "Development of methods for increasing the conversion efficiency and increasing the power of a multi-level power inverter" funded by the Ministry of Science and Higher Education of the Republic of Kazakhstan. His current research interests include power converter topologies, power converter control, renewable energy, and energy efficiency. He can be contacted at email: ssmoldahmetov@ku.edu.kz.



Makhabbat Krivolapova    graduated from the specialty physics and computer science and received a master of science degree in physics from the M. Kozybayev North-Kazakhstan University, Petropavlovsk, Kazakhstan, in 2007 and 2019, respectively. In 2020-2023, she studied for a doctorate at the M. Kozybayev North-Kazakhstan University, Petropavlovsk, Kazakhstan. Her current research interests include uninhabited submersibles, adaptive control, energy efficiency, and educational research in forestry. She can be contacted at email: krivolapovamakhabbat@gmail.com.